

**NANO EXPRESS**

**Open Access**

# Novel thin-GaN LED structure adopted micro abraded surface to compare with conventional vertical LEDs in ultraviolet light

Yen Chih Chiang<sup>1</sup>, Chien Chung Lin<sup>2\*</sup> and Hao Chung Kuo<sup>3\*</sup>

## Abstract

In this study, novel thin-GaN-based ultraviolet light-emitting diodes (NTG-LEDs) were fabricated using wafer bonding, laser lift-off, dry etching, textured surface, and interconnection techniques. Placing PN electrodes on the same side minimized the absorption caused by electrodes in conventional vertical injection light-emitting diodes (V-LEDs) and the current spreading was improved. The light output power (700 mA) of the NTG-LEDs was enhanced by 18.3% compared with that of the V-LEDs, and the external quantum efficiency (EQE) of the NTG-LEDs was also relatively enhanced by 20.0% compared with that of a reference device. When the current operations were 1,500 mA, the enhancements of the light output power and EQE were 27.4% and 27.2%, respectively. Additionally, the efficiency droop was improved by more than 15% at the same current level.

**Keywords:** Gallium nitride; Light-emitting diode; Vertical injection; Ultraviolet; Textured surface

## Background

A wide range of applications use ultraviolet (UV) lamps as a light source. These applications, such as chemical ink curing, disease or virus inspection, and air/water purification, traditionally adapt mercury-based lamps that are not environmentally friendly. To replace these mercury-based units, nitride-based UV light-emitting diodes (UV-LEDs) have recently received considerable attention because of their light-weight, high-efficiency, and eco-friendly features [1-4]. However, currently, the traditional nitride-based UV-LEDs cannot attain extremely high efficiency. Several improvements, such as AlInGaN barriers, high-temperature grown AlN buffers, pattern sapphire substrates, and current blocking layers, involving wafer epitaxy and layer designs have been proposed [5-10]. Apart from wafer design and quality problems, the sapphire-based UV-LEDs are influenced by the poor thermal dissipation of substrates and low light extraction efficiency [11-13]. Vertical injection

LEDs (V-LEDs) have been recently demonstrated as one of the most promising technologies for achieving superior brightness operation because of their excellent thermal dissipation [14-20]. In addition to thermal problems, to strengthen the light extraction efficiency, the surfaces of the V-LEDs are abraded to enable extra scattering capability [21-26]. Furthermore, the current V-LED metal-contact design affords extra absorption because of layouts and materials. In this study, a novel layout design combined with innovative fabrication processes facilitated placing p and n contact metals on the same side of the main LED lighting area; this effectively eliminated the aforementioned electrode absorption loss and maintained the advantages of vertical bonding architecture. In the following sections, novel thin-GaN-based ultraviolet light-emitting diodes (NTG-LEDs) that include such designs and were created through advanced processing techniques (such as wafer bonding, laser lift-off (LLO), dry etching, textured surface, and interconnection processes) are described.

## Methods

In this study, LED wafers were produced by depositing low-pressure metal-organic chemical vapor (LP-MOCVD) onto c-face (0001) 2-in.-diameter sapphire substrates. The

\* Correspondence: chienchunglin@faculty.nctu.edu.tw; hckuo@faculty.nctu.edu.tw

<sup>2</sup>Institute of Photonic System, National Chiao Tung University, No.301, Gaofa 3rd Rd., Guiren Dist., Tainan City 71150, Taiwan

<sup>3</sup>Department of Photonics and Institute of Electro-Optical Engineering, National Chiao Tung University, 1001 University Road, Hsinchu 300, Taiwan  
Full list of author information is available at the end of the article

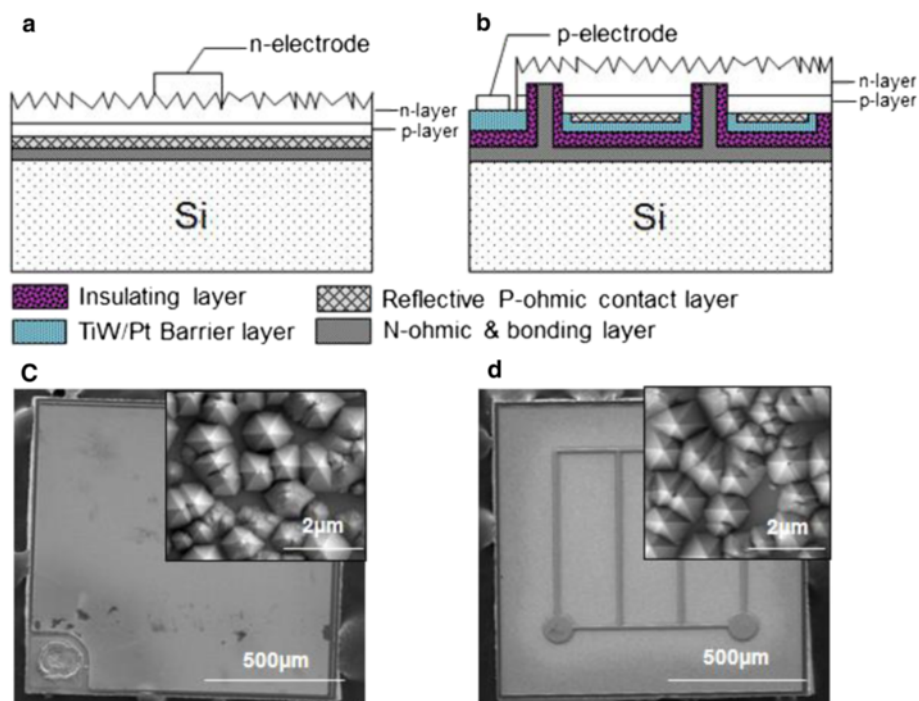


**Figure 1** Schematic diagrams and scanning electron microscope images of devices. (a, b) Both configurations and (c, d) SEM observations include appearances and micro abraded surface morphologies (insets).

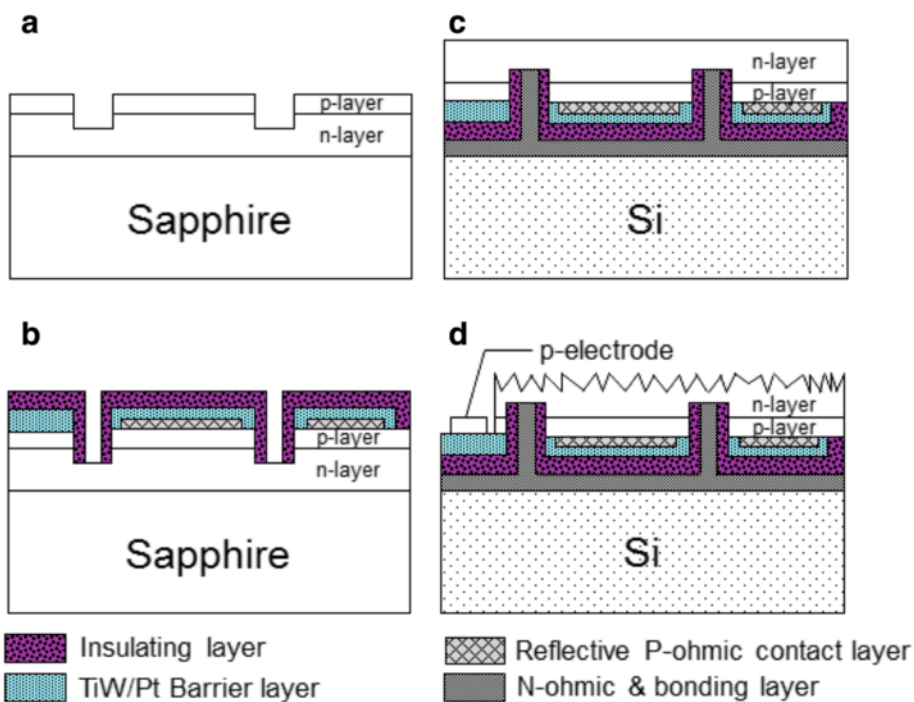
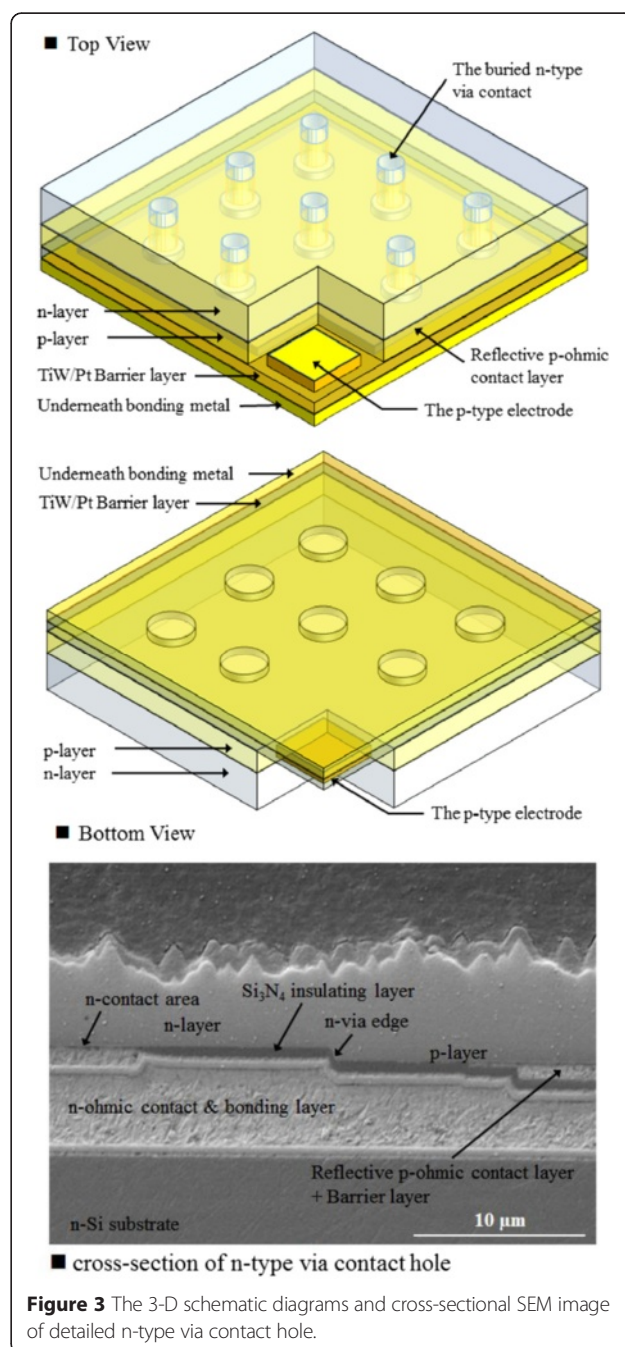


**Figure 2** Process flows of NTG-LEDs. (a) Defined the n-contact area, (b) n-area exposed from insulating layer (c) transferred the structure to silicon (d) abraded n-surface and deposited the p-electrode.

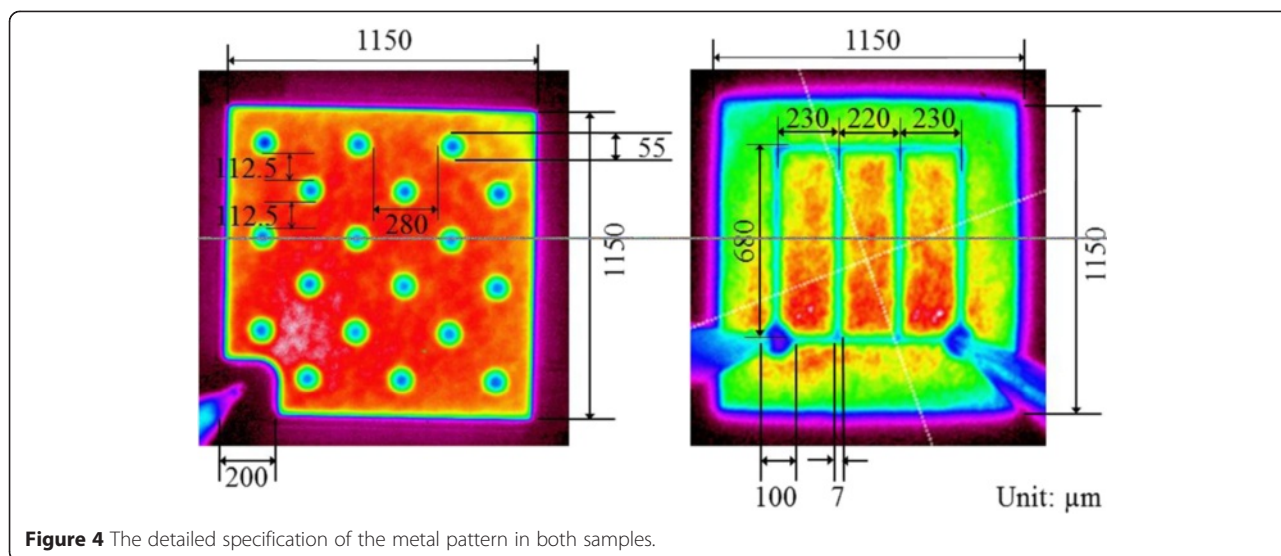
LED structure comprised a 20-nm-thick GaN nucleation layer, 0.5- $\mu\text{m}$ -thick undoped GaN layer, 2.0- $\mu\text{m}$ -thick Si-doped n-type AlGaIn cladding layer, unintentionally doped active region of 365-nm emitting wavelengths with six periods of InGaIn-AlGaIn multiple quantum wells (MQWs), 0.2- $\mu\text{m}$ -thick Mg-doped p-type GaN cladding layer, and Si-doped n-InGaIn-GaN short period superlattice structure.

Figure 1 shows a schematic diagram of conventional V-LEDs and NTG-LEDs. The fabrication processes of the NTG-LEDs were began to define the several n-contact vias by using an inductively couple plasma (ICP) to etch through the MQW to the n-GaN by an ICP etcher. After removing the photo-resist, a highly reflective ohmic contact layer of Ni (3 Å)/Ag (2,000 Å)/Ti (300 Å)/Pt (800 Å) was deposited on the blank wafer with n-contact vias and treated by 30-min thermal annealing at 430°C. In our design, the transparent conductive layer (TCL) which usually consists of indium tin oxide (ITO) is eliminated due to the light extraction concerns and flip-chip package layout. The TCL is favorable in conventional lateral blue LED fabrication, and it provides a highly transparent and conductive window for the p-side contact. However, in our devices, the less conductivity of the p-side contact was flip-chip bonded on a metal layer; thus, the current spreading was not an issue for the p-side conductivity. Furthermore, the emission wavelength was demonstrated in the UV region, where the TCL can absorb as high as 40% of the incident photons. Based on these two assessments, the TCL configuration was not included in our design. Subsequently, a metallic barrier layer of TiW (1,200 Å)/Pt (500 Å) was deposited and covered on the previous metal layer to prevent the subsequent silver from migrating to the PN junction, leading to the short circuiting of the device. An insulating layer of  $\text{Si}_3\text{N}_4$  (5,000 Å) was deposited on the entire surface through lithography and buffer oxide etchant (BOE) wet etching processes to expose the n-contact layer. Next, a Cr (300 Å)/Pt (500 Å)/Au (15,000 Å) bonding layer was evaporated to cover the gap and the entire area. The sample was then bonded onto a Cr (300 Å)/Pt (500 Å)/Au (15,000 Å)-coated n-type conducting Si substrate at 350°C for 1 h to form the flip-chip configuration illustrated in Figure 1b. The bonded samples were subsequently subjected to the LLO process to remove the sapphire substrate. A KrF excimer laser at a wavelength of 248 nm and with a pulse width of 25 ns was used to withdraw the sapphire substrate. The laser with a beam size of 0.3 mm  $\times$  0.3 mm was incident from the polished backside of the sapphire substrate onto the sapphire-GaN interface to decompose GaN into Ga and N. After removing the sapphire substrate, the samples were dipped into a HCl solution to eliminate the residual Ga from the u-GaN. Details of the LLO process are described in [17].

The u-GaN was then etched away to reveal the n-AlGaIn layer by using an ICP dry etcher; a square mesa (1,150  $\mu\text{m} \times 1,150 \mu\text{m}$ ) was created using ICP for current isolation purposes. To improve light output power and further enhance the light extraction efficiency of the NTG-LEDs, a micrometer-range random abraded surface was formed on the n-AlGaIn by using a KOH solution at 80°C for 120 s. Finally, the p-electrode contact area was created through ICP etching, and the process was completed by depositing a Ti (300 Å)/Al (1,500 Å)/Ni (1,000 Å)/Au (10,000 Å) metal electrode. Figure 1c,d



**Figure 3** The 3-D schematic diagrams and cross-sectional SEM image of detailed n-type via contact hole.



**Figure 4** The detailed specification of the metal pattern in both samples.

illustrates the scanning electron microscope images of the V-LEDs and NTG-LEDs. The insets of Figure 1c,d illustrate that a micrometer abraded surface is created on both samples' emission area. Figure 2 shows a brief summary of the process flow. The three-dimensional schematic structure of NTG-LED with both views (top and bottom) and cross-sectional SEM image of detailed n-type via contact hole are illustrated in Figure 3.

Because of the considerable changes in the contact layout design, the light-emitting areas of the V-LED and NTG-LED must be compared. The metal grid width for n-electrode of the V-LED is 7 μm, and the diameter of via for n-type electrode of the NTG-LED is 55 μm. The detailed specification of the metal pattern is shown in Figure 4. According to these specifications, the percentage

of shadowing effect ( $R_{shadow}$ ) is defined, and it can be expressed as follows:

$$R_{shadow} = \frac{A_{non-emission}}{A_{emission}} \times 100\% \quad (1)$$

where  $R_{shadow}$  is the ratio of the shadowing effect,  $A_{non-emission}$  is the dark area due to the contact metal, and  $A_{emission}$  is the area of illumination.

The  $R_{shadow}$  of both devices were 3.3% (V-LEDs) and 6.3% (NTG-LEDs). The conventional V-LEDs exhibited substantial n-type metal on the top surface, whereas the n-contact layer of the NTG-LEDs was buried beneath the active region. Therefore, no obvious electrode was observed in the NTG-LEDs. As compared to V-LEDs,

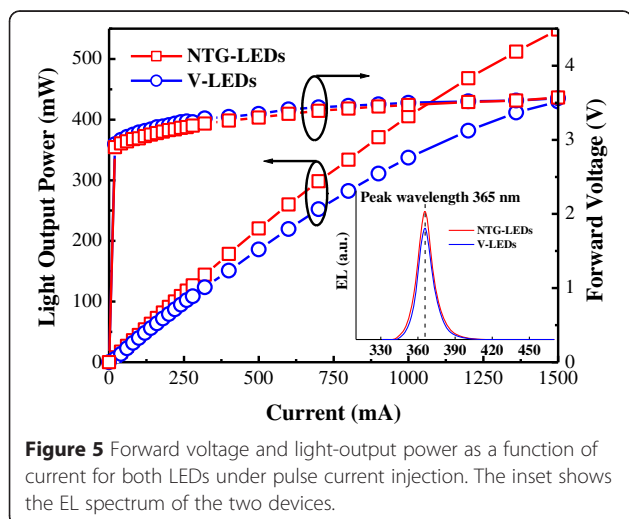


**Figure 5** Forward voltage and light-output power as a function of current for both LEDs under pulse current injection. The inset shows the EL spectrum of the two devices.

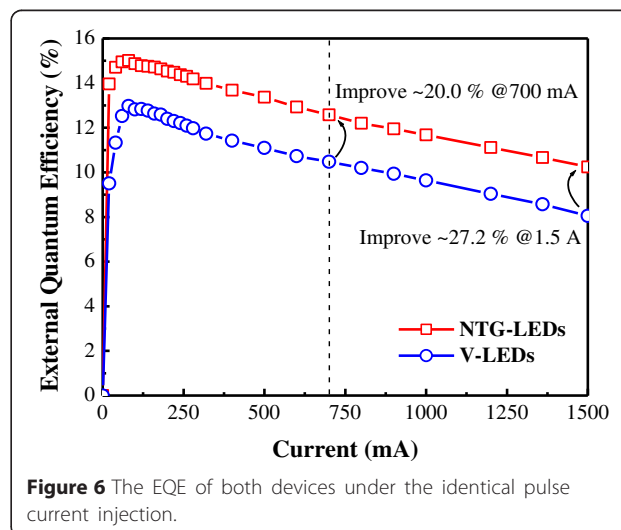


**Figure 6** The EQE of both devices under the identical pulse current injection.

NTG-LEDs only sacrificed a small corner of emission area to create the p-type contact area. This feature can reduced the packaging cost from requiring two gold wires to one gold wire and lower the absorption from fewer bonding pads and gold wires. In addition, the test results indicated that the output power of the NTG

samples substantially improved. Although the NTG samples had a higher shadowing factor than did the traditional V-LED, the distributed n-contact considerably facilitated the injection uniformity; thus, at the same pumping current, the overall output power of the NTG device was substantially stronger than that of the

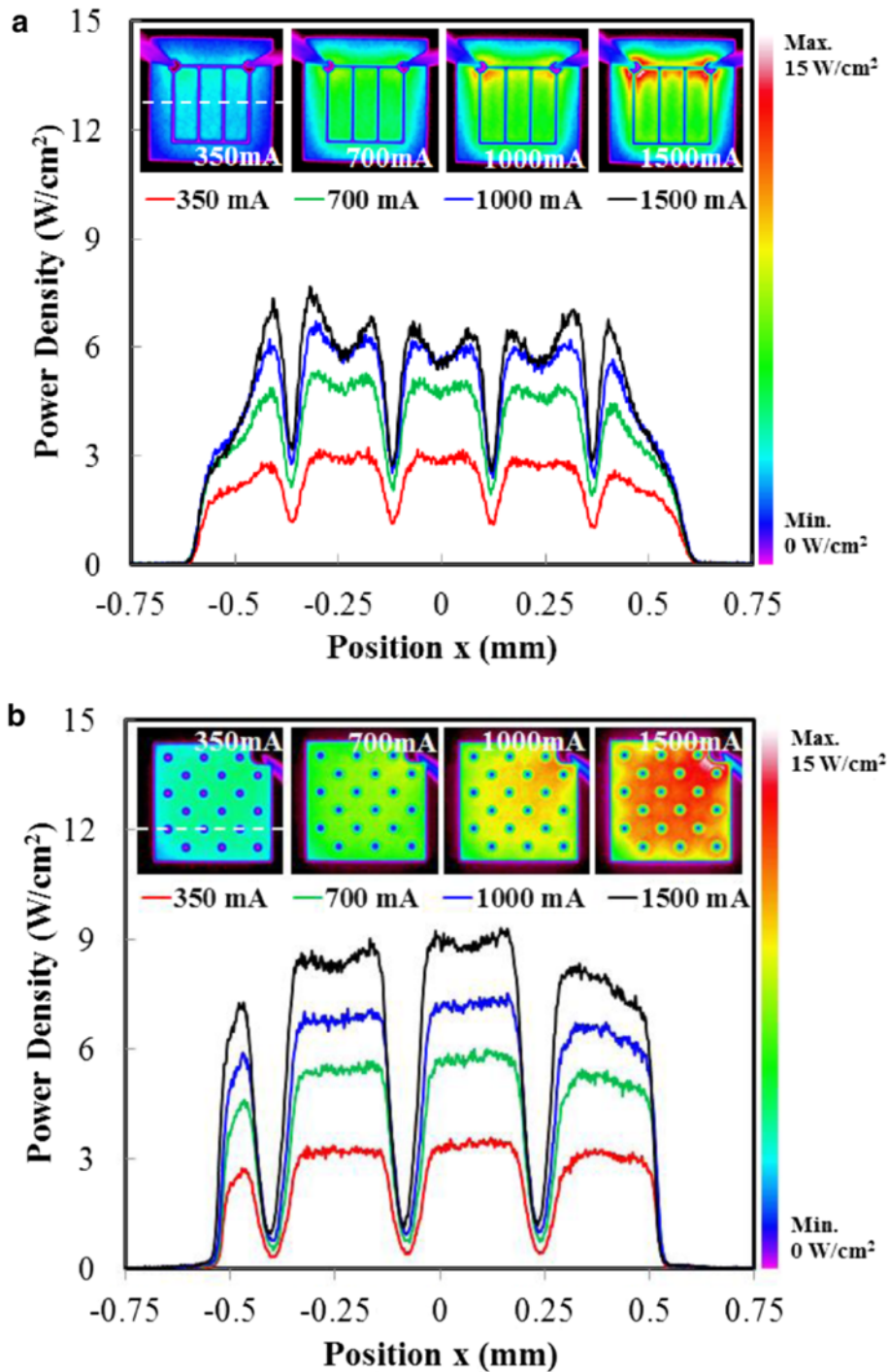


**Figure 7** Distributed light pattern demonstrated at different current injections and relation between position  $x$  and power density. (a) V-LEDs and (b) NTG-LEDs.

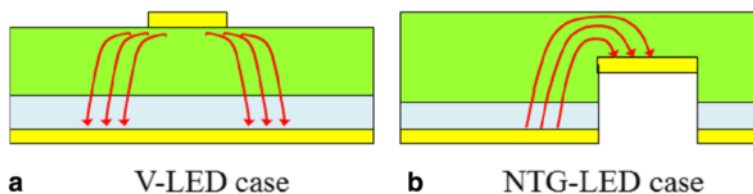


**Figure 8** The illustration of current spreading paths in different devices: (a) V-LED and (b) NTG-LED.

traditional V-LED. The optical and electrical characteristics were measured at room temperature by using a manual probing system featuring an integrating sphere detector and Keithley 2600 (Keithley Instruments Inc., Cleveland, OH, USA). To prevent the thermal effect during continuous DC current from causing a decrease in light-output power,  $L$ - $I$ - $V$  characteristics were measured under the pulse mode with a 2.5% duty cycle. The light intensity distribution and cross-sectional intensity profile were measured by Unice's LED beam profile detective system (Unice E-O Services Inc., Chungli, Taoyuan, Taiwan). Firstly, both samples were operated at 1,500 mA to fix the dark level/gain/threshold settings and then gradually reduce the current to measure the field distribution at the lower level of injection.

## Results and discussion

Figure 5 (inset) illustrates the electroluminescence (EL) spectra of both devices, indicating that the peak wavelength of both devices was at 365 nm. The EL intensity of the NTG-LEDs was higher than that of the reference device. According to the  $L$ - $I$ - $V$  characteristics shown in Figure 5, the  $I$ - $V$  curves for both devices were almost identical (approximately 3.25 V at 350 mA); this similarity indicates that the fabrication processes did not degrade the electrical properties of the devices. In addition, the  $L$ - $I$  characteristics indicate that the NTG-LEDs demonstrated more favorable linear characteristics during a high current injection than did the V-LEDs. When the current was 700 mA, the  $L$ - $I$ - $V$  characteristics (Figure 5) indicated that the measured intensity of the NTG-LEDs and reference device were 298 and 252 mW, respectively. When the current was continually increased to 1,500 mA, the power difference increased to 118 mW (548 mW for NTG-LEDs and 430 mW for V-LEDs).

Although the shadowing area of the NTG-LEDs was larger than that of the reference (6.3%:3.3%), the PN electrode layout induced a more favorable current spreading and led to an efficient output power. This condition enabled the NTG-LEDs to be enhanced substantially compared with the conventional V-LEDs [27-29].

As shown in Figure 6, the external quantum efficiency (EQE) was calculated according to the  $L$ - $I$ - $V$  characteristics. The EQE of the NTG-LEDs and reference device at the same 700- and 1,500-mA current injections were 12.6% and 10.5%, and 10.3% and 8.1%, respectively. Direct comparison was performed at the same injection levels, and the results indicated that the EQEs improved by 20.0% and 27.2% at 700 mA and 1,500 mA, respectively.

One of the major features of the proposed design is the improved current injection scheme. An efficient current spreading can lead to uniform light output and prevent the nonlinear crowding effect and eventual gain reduction. Figure 7 shows the light intensity distribution of the devices at various current levels. According to both the color-contoured planar map (insets) and the cross-sectional intensity profile, the NTG-LEDs exhibited a more favorable uniformity than did the V-LEDs. The basic current paths are different between the two cases, as can be seen in Figure 8. The case (a) (conventional V-LED) is more like the classical top contact structure which follows the current spreading formula [30]:

$$L_s = \sqrt{\frac{tn_{\text{ideal}}kT}{\rho J_0 e}} \quad (2)$$

where  $L_s$  is the characteristic spreading length,  $t$  is the thickness of the n-layer in our case,  $n_{\text{ideal}}$  is the ideality factor of the diode, and  $J_0$  is the current density at the edge of the metal contact.

**Table 1** Data of max. power, min. power, and uniformity in Figure 7

Current (mA)	Max. power (W/cm <sup>2</sup> )	Min. power (W/cm <sup>2</sup> )	U% (NTG)	Max. power (W/cm <sup>2</sup> )	Min. power (W/cm <sup>2</sup> )	U% VTF
350	3.508	3.166	5.1%	3.133	2.681	7.8%
700	5.873	5.337	4.8%	5.348	4.403	9.7%
1,000	7.463	6.662	5.7%	6.721	5.548	9.6%
1,500	9.224	8.178	6.0%	7.628	5.366	17.4%

On the other hand, the arrangement of electrodes in the case (b) (the NTG-LED) is very similar to the way we model the current crowding, and the corresponding spreading length ( $L_s$ ) is:

$$L_s = \sqrt{\frac{(\rho_c + \rho_p t_p) t_n}{\rho_n}} \quad (3)$$

where  $\rho_c$ ,  $\rho_p$ ,  $t_p$ ,  $\rho_n$ , and  $t_n$  are the p-type specific contact resistance, the resistivity and thickness of the p-type layer, and the resistivity and thickness of the n-type layer, respectively.

Comparing Equations 2 and 3, one can immediately observe the injection current dependence on Equation 2 brought by the term  $J_0$ . As the injection current increases, the  $L_s$  decreases. The reduction of  $L_s$  means the uneven distribution of the current, and thus, the intensity of light is getting worse. This phenomenon can be seen in the aforementioned beam profiles. Meanwhile, in Equation 3, the  $L_s$  is quite constant against the injection current, which can also be observed. Numerical analysis of maximal and minimal values across 0.7 mm of the center of the devices indicated the fair comparison of intensity uniformity. As shown in Table 1, the uniformity was calculated using the equation  $(\max - \min)/(\max + \min)$ . The NTG-LEDs exhibited a more favorable intensity uniformity than did the V-LEDs, particularly in high current ranges. The arrayed n-contact pattern improved the uniformity of the current injection, thus improving the resulting output light.

In addition to light output and current spreading, the efficiency droop of the devices was evaluated. The results indicated that the peak efficiency of both devices (V-LEDs and NTG-LEDs) were 13.0% and 15.0%, respectively. The efficiency droop ( $\eta$ ) can be expressed as:

$$\eta = \left( \frac{\eta_{\text{peak}} - \eta_{\text{exp}}}{\eta_{\text{peak}}} \right) \times 100\% \quad (4)$$

where  $\eta$  is the ratio of efficiency droop,  $\eta_{\text{peak}}$  is the maximum efficiency, and  $\eta_{\text{exp}}$  is the efficiency in different experimental currents.

The calculated droop percentages for both devices (NTG-LEDs and V-LEDs) at different current levels (at 700 and 1,500 mA) were 16.2% and 18.8%, and 31.7% and 37.7%, respectively. Therefore, the efficiency droop of the NTG-LEDs was enhanced by 16.0% and 18.9%, respectively, compared with that of the reference device. A uniform current injection can be attributed to this improvement [31].

## Conclusions

In summary, this paper presents a novel flip-chip architecture for UV-LEDs, called NTG-LEDs. Compared with

the conventional flip-chip structure, the configuration of the NTG-LEDs eliminated the electrode effect, increased the light extraction, and improved current spreading. According to the proposed device design, the light-output power of NTG-LEDs was further enhanced by 18.3% and 27.4% at 700- and 1,500-mA current levels, respectively. Furthermore, the EQE of the NTG-LEDs was effectively improved by 20.0% and 27.2% when 700 and 1,500 mA of current were supplied, respectively. Finally, the efficiency droop was improved by 16.0% and 18.9% at the same current level, respectively. Therefore, the proposed NTG-LED is promising for use in the next generation of UV-LEDs.

## Abbreviations

EL: electroluminescence; EQE: external quantum efficiency; ICP: inductively couple plasma; LLO: laser lift-off; LP-MOCVD: low-pressure metal-organic chemical vapor deposition; MQW: multiple quantum wells; NTG-LEDs: novel thin-GaN-based ultraviolet light-emitting diodes; UV: ultraviolet; UV-LEDs: UV light-emitting diodes; V-LED: vertical injection light-emitting diodes.

## Competing interests

The authors declare that they have no competing interests.

## Authors' contributions

YCC participated in the design of the study and fabricated and measured all the samples, explained all the measured data, and contributed in the writing of the manuscript. CCL participated in the revision of the manuscript and discussion of the results. HCK participated in the discussion of all the results. All authors read and approved the final manuscript.

## Acknowledgements

This work was supported in part by the National Science Council of Taiwan under grant numbers NSC101-2221-E-009-046-MY3, MOST103-2622-E-009-008-CC3, and MOST103-2120-M-110-003.

## Author details

<sup>1</sup>Institute of Lighting and Energy Photonics, National Chiao Tung University, No.301, Gaofa 3rd Rd., Guiren Dist., Tainan City 71150, Taiwan. <sup>2</sup>Institute of Photonic System, National Chiao Tung University, No.301, Gaofa 3rd Rd., Guiren Dist., Tainan City 71150, Taiwan. <sup>3</sup>Department of Photonics and Institute of Electro-Optical Engineering, National Chiao Tung University, 1001 University Road, Hsinchu 300, Taiwan.

Received: 30 January 2015 Accepted: 28 March 2015

Published online: 15 April 2015

## References

- Schubert EF, Kim JK. Solid-state light sources getting smart. *Science*. 2005;308:1274–8.
- Koike M, Shibata N, Kato H, Takahashi Y. Development of high efficiency GaN-based multi-quantum-well LEDs and their applications. *IEEE J Sel Topics Quantum Electron*. 2002;8:271–7.
- Khan A, Balakrishnan K, Katona K. Ultraviolet light-emitting diodes based on group three nitrides. *Nat Photonics*. 2008;2:77–84.
- Kneissl M, Kolbe T, Chua C, Kueller V, Lobo N, Stellmach J, et al. Advances in group III-nitride-based deep UV light-emitting diode technology. *Semicond Sci Technol*. 2011;26:014036-1–6.
- Tu PM, Chang CY, Huang SC, Chiu CH, Chang JR, Chang WT, et al. Investigation of efficiency droop for InGaN-based UV light-emitting diodes with InAlGaIn barrier. *Appl Phys Lett*. 2011;98:211107-1–3.
- Ohba Y, Kaneko K, Katsuno H, Kushibe M. Highly efficient InGaN-based 383-nm ultraviolet light-emitting diodes fabricated on sapphire substrate using high-temperature-grown AlN buffer. *Appl Phys Express*. 2008;1:101101-1–3.

7. Wang WK, Wu DS, Lin SH, Han P, Horng RH, Hsu TC, et al. Efficiency improvement of near-ultraviolet InGaN LEDs using patterned sapphire substrates. *IEEE J Quantum Electron*. 2005;41(11):1403–8.
8. Huh C, Lee JM, Kim DJ, Park SJ. Improvement in light-output efficiency of InGaN/GaN multiple-quantum well light-emitting diodes by current blocking layer. *J Appl Phys*. 2002;92(5):2248–50.
9. Adivarahan V, Chitnis A, Zhang JP, Shatalov M, Yang JW, Simin G, et al. Ultraviolet light-emitting diodes at 340 nm using quaternary AlInGaN multiple quantum wells. *Appl Phys Lett*. 2001;79:4240–2.
10. Wang T, Liu YH, Lee YB, Ao JP, Bai J, Sakai S. 1 mW AlInGaN-based ultraviolet light-emitting diode with an emission wavelength of 348 nm grown on sapphire substrate. *Appl Phys Lett*. 2002;81:2508–10.
11. Chang SJ, Lin YC, Su YK, Chang CS, Wen TC, Shei SC, et al. Nitride-based LEDs fabricated on patterned sapphire substrates. *Solid State Electron*. 2003;47:1539–42.
12. Horng RH, Hu HL, Lin RC, Tang LS, Hsu CP, Ou SL. Cup-shaped copper heat spreader in multi-chip high-power LEDs application. *Opt Express*. 2012;20(55):A597–605.
13. Horng RH, Hsiao HY, Chiang CC, Wu DS, Tsai YL, Lin HI. Novel device design for high-power InGaN/sapphire LEDs using copper heat spreader with reflector. *IEEE J Quantum Electron*. 2009;15:1281–6.
14. Wong WS, Sands T, Cheung NW, Kneissl M, Bour DP, Mei P, et al. InGaN light emitting diodes on Si substrates fabricated by Pd-In metal bonding and laser lift-off. *Appl Phys Lett*. 2000;77:2822–4.
15. Tan BS, Yuan S, Kang XJ. Performance enhancement of InGaN light-emitting diodes by laser lift-off and transfer from sapphire to copper substrate. *Appl Phys Lett*. 2004;84:2757–9.
16. Chu JT, Kuo HC, Kao CC, Huang HW, Chu CF, Lin CF, et al. Fabrication of p-side down GaN vertical light emitting diodes on copper substrates by laser lift-off. *Phys Stat Sol (c)*. 2004;1:2413–6.
17. Chu CF, Lai FI, Chu JT, Yu CC, Lin CF, Kuo HC, et al. Study of GaN light-emitting diodes fabricated by laser lift-off technique. *J Appl Phys*. 2004;95:3916–22.
18. Lin WY, Wu DS, Pan KF, Huang SH, Lee CE, Wang WK, et al. High-power GaN-mirror-Cu light-emitting diodes for vertical current injection using laser liftoff and electroplating techniques. *IEEE Photon Technol Lett*. 2005;17(9):1809–11.
19. Horng RH, Chen CH, Kao WC, Wu DS. High-yield thin GaN LED using metal bonding and laser lift-off technology. *Proc of SPIE*. 2012;84841H:1–6.
20. Guo EQ, Liu ZQ, Wang LC, Yi XY, Wang GH. Optical and electrical characteristics of GaN vertical light emitting diode with current block layer. *J Semicond*. 2011;32(6):064007-1–4.
21. Kao CC, Kuo HC, Yeh KF, Chu JT, Peng WL, Huang HW, et al. GaN laser lift-off light-emitting diodes formed by ICP dry etching. *IEEE Photon Technol Lett*. 2007;19:849–51.
22. Fujii KT, Gao Y, Sharma R, Hu EL, DenBaars SP, Nakamura S. Increase in the extraction efficiency of GaN-based light-emitting diodes via surface roughening. *Appl Phys Lett*. 2004;84:855–7.
23. Huang HW, Kao CC, Chu JT, Kuo HC, Wang SC, Yu CC. Improvement of InGaN-GaN light-emitting diode performance with a nano-roughened p-GaN surface. *IEEE Photon Technol Lett*. 2005;17:983–5.
24. Windisch R, Rooman C, Meinschmidt S, Kiesel P, Zipperer D, Döhler GH, et al. Impact of texture-enhanced transmission on high-efficiency surface-textured light-emitting diodes. *Appl Phys Lett*. 2001;79:2315–7.
25. Lee YJ, Kuo HC, Lu TC, Wang SC. High light-extraction GaN-based vertical LEDs with double diffuse surface. *IEEE J Quantum Electron*. 2006;42:1196–10.
26. Huh C, Lee KS, Kang EJ, Park SJ. Improved light-output and electrical performance of InGaN-based light-emitting diode by microroughening of the p-GaN surface. *J Appl Phys*. 2003;93:9383–5.
27. Kudryk YY, Zinovchuk AV. Efficiency droop in InGaN/GaN multiple quantum well light-emitting diodes with nonuniform current spreading. *Semicond Sci Technol*. 2011;26(9):095007-1–5.
28. Liu GY, Zhang J, Tan CK, Tansu N. Efficiency-droop suppression by using large-bandgap AlGaInN thin barrier layers in InGaN quantum-well light-emitting diodes. *IEEE Photonics J*. 2013;5(2):2201011-1–2201011-11.
29. Bogdanov MV, Bulashevich KA, Khokhlev OV, Evstratov IY, Ramm MS, Karpov SY. Current crowding effect on light extraction efficiency of thin-film LEDs. *Phys Stat Solidi*. 2010;7(7–8):2124–6. c.
30. Schubert EF. *Light emitting diodes*. 2nd ed. Cambridge: Cambridge University Press; 2006.
31. Li CK, Wu YR. Study on the current spreading effect and light extraction enhancement of vertical GaN/InGaN LEDs. *IEEE Trans Electron Devices*. 2012;59(2):400–7.

**Submit your manuscript to a SpringerOpen<sup>®</sup> journal and benefit from:**

- Convenient online submission
- Rigorous peer review
- Immediate publication on acceptance
- Open access: articles freely available online
- High visibility within the field
- Retaining the copyright to your article

---

Submit your next manuscript at ► [springeropen.com](http://springeropen.com)

---